

A Fault Tolerance Mechanism for UAV-Assisted Vehicular Network in Disaster Rescue

1st Kaiqi Zhang

Dalian University of Technology
Dalian, China
zhangkq@mail.dlut.edu.cn

2nd Jing Zhao*

Dalian University of Technology
Dalian, China
zhaoj9988@mail.dlut.edu.cn

3rd Rui Chen

Dalian University of Technology
Dalian, China
72117004@mail.dlut.edu.cn

Abstract—Data sharing among ground rescue vehicles is essential for safe and efficient operations in disaster-stricken areas. When disasters disrupt communication infrastructure, unmanned aerial vehicles (UAVs) can be deployed to facilitate data sharing among vehicles. However, maintaining reliable inter-vehicle communication is challenging due to potential UAV and link failures. To enhance communication reliability, we propose a fault tolerance mechanism for UAV-assisted vehicular networks. We introduce the novel concept of K-fault tolerance, which marks the first study of fault tolerance in this context. Moreover, we develop a UAV deployment algorithm that minimizes UAV requirements, controlling costs while maintaining K-fault tolerance. Furthermore, we propose a fault tolerance topology control algorithm (FTTCA) that adjusts deployed UAV communication ranges to further reduce costs while ensuring K-fault tolerance, supported by corresponding theorem proofs. Extensive simulations validate the effectiveness of our proposed UAV deployment algorithm and FTTCA and demonstrate the superiority of our fault tolerance mechanism in managing UAV and link failures.

Index Terms—Unmanned aerial vehicle (UAV), fault tolerance, UAV deployment algorithm, topology control algorithm.

I. INTRODUCTION

Natural disasters, including earthquakes, flash floods, and tsunamis, can cause substantial damage to property and loss of human life. In disaster-affected regions, vehicles need to exchange crucial information, including rescue instructions, road condition assessments, and real-time traffic updates, to facilitate post-disaster recovery and enhance road safety [1]. Recent advancements in communication technologies have propelled the evolution of the Internet of Vehicles (IoV), which enhances the efficiency and safety of numerous vehicular services and applications [2]. Nevertheless, the destruction of critical infrastructure during disasters, such as damage to cellular base stations, Wi-Fi access points, and power grids, can significantly degrade or disrupt wireless services, compromising IoV functionality [3].

Recently, UAVs have garnered significant attention due to their cost-effectiveness, agile maneuverability, and line-of-sight (LoS) communication capabilities. Furthermore, leveraging air-to-air (A2A) and air-to-ground (A2G) communications, multiple UAVs can facilitate data sharing among vehicular networks even without communication infrastructure. Extensive research has focused on optimizing UAV-assisted

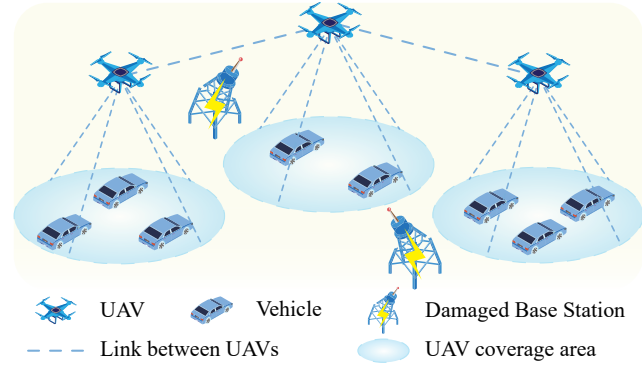


Fig. 1: Motivation: In UAV-assisted vehicular networks without base stations or fault tolerance, a single UAV or link failure can critically disrupt communication, creating a vulnerability.

aerial-ground networks to enhance disaster rescue operations. Shakhatreh et al. [4] proposed deploying UAVs as airborne wireless base stations in the absence of cellular networks and optimized UAV positions to maximize uplink transmission time. Su et al. [5] introduced a lightweight, blockchain-enabled secure data sharing framework for UAV-assisted IoV to address security threats and challenges in disaster scenarios.

Despite advancements in network and algorithm design, research on fault tolerance in UAV-assisted vehicular networks remains limited. Unexpected UAV malfunctions and communication link failures can disrupt information transmission, significantly impeding vehicle communication during disaster rescue operations and compromising the efficiency and reliability of data sharing in UAV-assisted vehicular networks, as illustrated in Fig. 1. Consequently, developing a robust fault tolerance mechanism for UAV-assisted vehicular networks is crucial to ensure reliable inter-vehicle communication and enhance the efficiency of rescue operations in disaster scenarios.

Fault tolerance mechanisms enhance system reliability by employing backup systems, error correction technologies, and redundant links. Recent research has focused on enhancing Byzantine algorithms [6] and exploring more efficient hypercube structures [7] for fault tolerance mechanisms. However, the Byzantine algorithm, which requires extensive message passing, and the uniform hypercube structure are not well-suited for UAV-assisted vehicular networks characterized by limited communication resources and dynamic topology. Con-

Jing Zhao* is corresponding author.

sequently, developing an efficient and adaptive fault tolerance mechanism for UAV-assisted vehicular networks remains a significant challenge in this field.

To address these challenges, this paper proposes a novel fault tolerance mechanism for UAV-assisted vehicular networks, designed to ensure reliable communication and enhance rescue efficiency in disaster scenarios. We introduce the concept of K -fault tolerance, specifically tailored to the unique characteristics of UAV-assisted vehicular networks. We then propose a UAV deployment algorithm that optimizes UAV utilization and minimizes operational costs while meeting fault tolerance requirements. Finally, we present the FTTCA, which further reduces costs by optimizing the communication ranges of deployed UAVs while maintaining the required level of fault tolerance, accompanied by a proof of concept.

Our contributions can be summarized as follows:

- 1) We define K -fault tolerance for UAV-assisted vehicular networks, which, to the best of our knowledge, represents the first study addressing fault tolerance in this specific context.
- 2) We propose a UAV deployment algorithm that iteratively eliminates redundant UAVs to minimize their number while ensuring K -fault tolerance, thereby optimizing costs and maintaining network performance.
- 3) We present the FTTCA, which utilizes K disjoint paths of internal nodes and includes a corresponding theorem proof. This algorithm optimizes the communication ranges of deployed UAVs to minimize operational costs while maintaining K -fault tolerance.
- 4) We validate the effectiveness of the proposed fault tolerance mechanism through extensive simulations. The results demonstrate the superiority of UAV deployment algorithm and FTTCA over existing schemes in managing UAV and communication link failures.

II. SYSTEM MODEL AND DEFINITIONS

This section delineates the system model for UAV-assisted vehicular networks, provides definitions of key symbols, and introduces the concept of K -fault tolerance.

A. System Model

As illustrated in Fig. 2, we assume that all base stations (BSs) within the affected region become inoperative during a sudden natural disaster. A set of UAVs, denoted as $U = \{u_1, u_2, \dots, u_m\}$, is deployed to facilitate communication for a set of vehicles, denoted as $V = \{v_1, v_2, \dots, v_n\}$. Each vehicle conducts rescue missions within its designated operational area, represented by the set $R = \{r_1, r_2, \dots, r_n\}$. For clarity, v will denote both the vehicle and its corresponding location.

Communication within the UAV-assisted vehicular network encompasses both UAV-to-UAV and UAV-to-vehicle channels.

1) *UAV-to-UAV (A2A) Channel:* UAV-to-UAV communication primarily relies on LoS links [8], utilizing the free space propagation loss model to estimate path loss.

$$L_{u,\tilde{u}} = 20 \log D_{u,\tilde{u}} + 20 \log f_0 + 20 \log(4\pi/c) \quad (1)$$

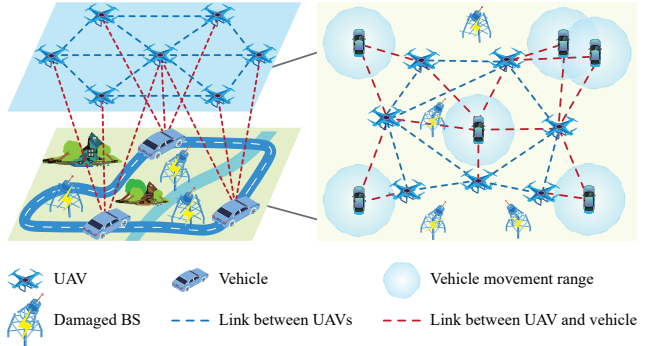


Fig. 2: Network model of a UAV-assisted vehicular network in a disaster-stricken area.

Here, $D_{u,\tilde{u}}$ represents the Euclidean distance between UAV u and \tilde{u} , f_0 denotes the carrier frequency, and c is the speed of light. Assuming a uniform maximum transmission power P_s for all UAVs, the maximum A2A communication range, R_{max}^{A2A} , can be derived [9].

2) *UAV-to-Vehicle (A2G) Channel:* Our A2G communication model incorporates both LoS and Non-Line-of-Sight (NLoS) links, which are influenced by environmental factors. Each vehicle establishes a connection with a UAV via either a LoS or an NLoS link, with these transmissions being statistically independent [10]. NLoS links are subject to significant signal attenuation and multipath effects, resulting in reduced reliability and lower data rates. Consequently, our model prioritizes LoS links to maintain high-quality A2G communications.

The establishment of a LoS link is determined by the elevation angle $\theta_{v,u}$ between the vehicle v and the UAV u , based on the principles of the first Fresnel zone [11]. A threshold elevation angle σ is defined for LoS communication: if $\theta_{v,u} \geq \sigma$, a LoS link is established; otherwise, an NLoS link forms. The maximum communication radius for LoS links, R_{max}^{A2G} , is derived from the UAV altitude Z as $R_{max}^{A2G} = \frac{Z}{\tan \sigma}$.

B. Definitions

Table I summarizes the primary notations used in this paper.

In the network topology G , communication fault tolerance between any two vehicles is categorized into three distinct types: vertex, edge, and path.

- *K -Vertex Fault Tolerance:* Vertex fault tolerance evaluates the impact of removing up to $K - 1$ UAVs on the connectivity between vehicles v and \tilde{v} in G . If communication persists uninterrupted despite these UAV failures, then $v \Rightarrow \tilde{v}$ achieves K -vertex fault tolerance.
- *K -Edge Fault Tolerance:* Edge fault tolerance determines the effect of up to $K - 1$ link failures on the connectivity between vehicles v and \tilde{v} in G . If communication remains stable despite these link failures, then $v \Rightarrow \tilde{v}$ possesses K -edge fault tolerance.
- *K -Path Fault Tolerance:* If at least K distinct paths exist between vehicles v and \tilde{v} , then $v \Rightarrow \tilde{v}$ demonstrates K -path fault tolerance. Should any path fail or become congested, v can utilize up to $K - 1$ alternative paths, facilitating multi-path routing and load balancing.

TABLE I: Symbol Definition

Symbol	Definitions
$A = [A_u]_{1 \times m}$	A binary matrix representing the states of UAVs.
$B = [B_{v,u}]_{n \times m}$	A matrix recording the horizontal distances between vehicle v and UAV u .
$C = [C_{v,u}]_{n \times m}$	A binary matrix representing the LoS associations between vehicles and UAVs.
$D = [D_{u,\tilde{u}}]_{m \times m}$	A symmetric matrix measuring the Euclidean distances between pairs of UAVs.
$E = [E_{u,\tilde{u}}]_{m \times m}$	A symmetric binary matrix indicating the communication associations between UAVs.
$\langle u, v \rangle / \langle u, \tilde{u} \rangle$	A directed A2G/A2A link from UAV u to vehicle v /UAV \tilde{u} .
$u \rightarrow \tilde{u}$	UAV u and \tilde{u} can communicate directly in one hop, or there exists a directed A2A link $\langle u, \tilde{u} \rangle$.
$u \rightarrow v$	UAV u and vehicle v can communicate directly in one hop, or there exists a directed A2G link $\langle u, v \rangle$.
$u \Rightarrow \tilde{u}$	UAV u and \tilde{u} can communicate directly ($u \rightarrow \tilde{u}$) or indirectly.
$u \Rightarrow v$	UAV u and vehicle v can communicate directly ($u \rightarrow v$) or indirectly.
$v \Rightarrow \tilde{v}$	Vehicle v and vehicle \tilde{v} can communicate with each other through UAVs.
pd	A ringless path in network topology.
$V(pd)$	The set of UAVs and vehicles along pd .
$E(pd)$	The set of A2A and A2G links along pd .
$V(G_0)/V(G_F)$	The sets of UAVs and vehicles in G_0/G_F , respectively.
$E(G_0)/E(G_F)$	The sets of A2A and A2G links between UAVs in G_0/G_F , respectively.
$R_{max}^{A2A}/R_{max}^{A2G}$	The maximum communication radius for A2A/A2G communication of UAVs, assuming all UAVs have the same $R_{max}^{A2A}/R_{max}^{A2G}$.
G_0	The network topology where each UAV uses the $R_{max}^{A2A}/R_{max}^{A2G}$ communication radius. $\forall \langle u, \tilde{u} \rangle, \langle u, v \rangle \in E(G_0)$, the conditions $D_{u,\tilde{u}} \leq R_{max}^{A2A}$ and $B_{v,u} \leq R_{max}^{A2G}$ are satisfied.
$N_A(u)/N_G(u)$	The one-hop neighboring UAVs/vehicles of UAV u in G_0 , corresponding to the adjacency points of A2A/A2G links for UAV u .
R_u^{A2A}/R_u^{A2G}	The selected A2A/A2G communication radius for UAV u after fault-tolerant topology control. $R_u^{A2A} \in (0, R_{max}^{A2A})$, and $R_u^{A2G} \in (0, R_{max}^{A2G})$. The topology structure after fault tolerant topology control. Clearly, $V(G_F) = V(G_0)$ and $E(G_F) \subseteq E(G_0)$.
G_F	
$N_A^F(u)/N_G^F(u)$	The one-hop neighboring UAVs/vehicles that need to communicate with UAV u directly in G_F . For any $\tilde{u} \in N_A^F(u)$, $D_{u,\tilde{u}} \leq R_u^{A2A} \leq R_{max}^{A2A}$, and $N_A^F(u) \subseteq N_A(u)$. Similarly, $\forall v \in N_G^F(u)$, $B_{v,u} \leq R_u^{A2G} \leq R_{max}^{A2G}$, and $N_G^F(u) \subseteq N_G(u)$.

Specifically, if network G maintains K -vertex, K -edge, and K -path fault tolerance simultaneously for all vehicle pairs, then it achieves comprehensive K -fault tolerance.

III. UAV DEPLOYMENT ALGORITHM WITH K -FAULT TOLERANCE

The proposed UAV deployment algorithm determines the minimum number of UAVs required to achieve K -fault tolerance within a specified area.

A. Problem Formulation

Consider a rectangular region with dimensions L (length) and W (width) containing n vehicles and m UAVs. $A_u = 1$ represents an active UAV, whereas $A_u = 0$ represents a

deactivated UAV. $C_{v,u} = 1$ indicates that vehicle v is within the LoS range of UAV u ($B_{v,u} \leq R_u^{A2G}$), whereas $C_{v,u} = 0$ indicates otherwise. $E_{u,\tilde{u}} = 1$ if $D_{u,\tilde{u}} \leq R_u^{A2A}$; otherwise, $E_{u,\tilde{u}} = 0$. The UAV deployment problem can then be formulated mathematically as shown in Equation 2.

$$\begin{aligned}
& \min \sum_{u \in U} A_u, \\
s.t. \quad & C_1: \forall v \in V, \forall u, \tilde{u} \in U, A_v, C_{v,u}, E_{u,\tilde{u}} \in \{0, 1\}, \\
& C_2: \forall v \in V, \forall u, \tilde{u} \in U, 0 \leq B_{v,u}, D_{u,\tilde{u}} \leq \sqrt{L^2 + W^2}, \\
& C_3: \forall u, \tilde{u} \in U, D_{u,\tilde{u}} = D_{\tilde{u},u}, E_{u,\tilde{u}} = E_{\tilde{u},u}, \\
& C_4: \forall u \in U, A_u = 0, \\
& \sum_{\tilde{u} \in U} E_{u,\tilde{u}} = \sum_{\tilde{u} \in U} E_{\tilde{u},u} = 0, \sum_{v \in V} C_{v,u} = 0, \\
& C_5: \forall u, \tilde{u} \in \tilde{U}, u \neq \tilde{u}, D_{u,\tilde{u}} \geq R_{MHC}, \\
& C_6: \forall v, \tilde{v} \in V, \forall v \in r, \forall \tilde{v} \in \tilde{r}, \exists \rho \geq 0, \exists u, \tilde{u} \in \tilde{U} \setminus \binom{\tilde{U}}{K-1}, \\
& A_{\binom{\tilde{U}}{K-1}} = 0, C_{v,u}(E^\rho)_{u,\tilde{u}} C_{\tilde{v},\tilde{u}} > 0, \\
& C_7: \forall v, \tilde{v} \in V, \forall v \in r, \forall \tilde{v} \in \tilde{r}, \exists \rho \geq 0, \exists u, \tilde{u} \in \tilde{U}, \\
& C_{\binom{\{<v,u>|C_{v,u}=1\}}{Q}} = E_{\binom{\{<u,\tilde{u}>|E_{v,u}=1\}}{Q}} = 0, \\
& 0 \leq Q < K, Q \in N, C_{v,u}(E^\rho)_{u,\tilde{u}} C_{\tilde{v},\tilde{u}} > 0, \\
& C_8: \forall v, \tilde{v} \in V, \forall v \in r, \forall \tilde{v} \in \tilde{r}, \forall u, \tilde{u} \in \tilde{U}, \\
& \sum_{\rho=0}^{m-1} C_{v,u}(E^\rho)_{u,\tilde{u}} C_{\tilde{v},\tilde{u}} \geq K,
\end{aligned} \tag{2}$$

Here, \tilde{U} represents the set of reserved UAVs. R_{MHC} represents the minimum allowable distance between UAVs. $\binom{\tilde{U}}{K-1}$ denotes the combination of selecting any $K-1$ UAVs from the set \tilde{U} . Additionally, $\binom{\{<v,u>|C_{v,u}=1\}}{Q} \cup \binom{\{<u,\tilde{u}>|E_{v,u}=1\}}{Q}$ refers to the selection of $K-1$ links, encompassing both A2G and A2A connections. Furthermore, E^ρ quantifies the number of ρ -hop paths connecting any two UAVs in \tilde{U} .

B. Algorithm Design

The UAV deployment optimization problem, as formulated in Equation 2, is NP-hard. This computational complexity makes finding the optimal solution particularly challenging, especially in large-scale scenarios. Consequently, we propose a heuristic algorithm that iteratively removes redundant UAVs to approximate the optimal solution efficiently.

The proposed algorithm consists of three main processes:

Process 1: To achieve K -fault tolerance, candidate UAVs are initially deployed at every intersection point across the $L \times W$ grid, ensuring comprehensive coverage. Initially, all entries in matrix A are set to 1, indicating that all UAVs are active, while the set \tilde{U} of reserved UAVs is initialized as empty. Subsequently, the values for matrices B , C , D , and E are calculated based on the initial deployment configuration.

Process 2: To ensure secure and stable operation, a minimum safety distance is maintained between UAVs [12]. The Matérn III hard-core point process [13] is employed to iteratively identify and remove UAVs violating this requirement. Initially, an active UAV is randomly selected, with priority given to those having shorter collective distances to vehicles V and reserved UAVs \tilde{U} , ensuring convergence and optimality.

Algorithm 1: Determine whether UAV u is redundant for U/\tilde{U} (using U as an example).

Input: V, U, A, C, E
Output: A Boolean value

- 1 $A_u \leftarrow \sum_{\tilde{u} \in U} E_{u,\tilde{u}} \leftarrow \sum_{\tilde{u} \in U} E_{\tilde{u},u} \leftarrow \sum_{v \in V} C_{v,u} \leftarrow 0;$
- 2 **for** $v \in V$ **&&** $\tilde{v} \in V$ **do**
- 3 // for each vehicle position
- 4 **for** $v \in r$ **&&** $\tilde{v} \in \tilde{r}$ **do**
- 5 ▷ **K-Vertex Fault Tolerance**
- 6 **for** $1 : \binom{m}{K-1}$ **do**
- 7 $A_{(\tilde{K}-1)} \leftarrow \sum_{v \in V} C_{v,(\tilde{K}-1)} \leftarrow 0;$
- 8 $\sum_{\tilde{u} \in U} E_{(\tilde{K}-1),\tilde{u}} \leftarrow \sum_{\tilde{u} \in U} E_{\tilde{u},(\tilde{K}-1)} \leftarrow 0;$
- 9 **if** $\#\rho \geq 0$, $\forall u_1, u_2 \in U \setminus (\tilde{K}-1), C_{v,u_1}(E^\rho)_{u_1,u_2} C_{\tilde{v},u_2} > 0$ **then**
- 10 | **return False;**
- 11 **end**
- 12 **end**
- 13 ▷ **K-Edge Fault Tolerance**
- 14 Let l be the number of links in
- 15 $\{<v,u> | C_{v,u} = 1\} \cup \{<u,\tilde{u}> | E_{v,u} = 1\};$
- 16 **for** $1 : \binom{l}{K-Q-1}$ **do**
- 17 $C_{(\tilde{K}-Q-1)} \leftarrow E_{(Q)} \leftarrow 0;$
- 18 **if** $\#\rho \geq 0$,
- 19 $\forall u_1, u_2 \in U, C_{v,u_1}(E^\rho)_{u_1,u_2} C_{\tilde{v},u_2} > 0$
- 20 **then**
- 21 | **return False;**
- 22 **end**
- 23 **end**
- 24 ▷ **K-Path Fault Tolerance**
- 25 $\gamma \leftarrow 0;$
- 26 **for** $\rho \leftarrow 0 : m - 1$ **do**
- 27 **if** $\exists u_1, u_2 \in U, C_{v,u_1}(E^\rho)_{u_1,u_2} C_{\tilde{v},u_2} > 0$
- 28 **then**
- 29 | $\gamma \leftarrow \gamma + C_{v,u_1}(E^\rho)_{u_1,u_2} C_{\tilde{v},u_2};$
- 30 **end**
- 31 **if** $\gamma < K$ **then**
- 32 | **return False;**
- 33 **end**
- 34 **end**
- 35 **return True**

To prevent infinite loops, a probabilistic factor is incorporated into the UAV selection process, as shown in Equation 3, introducing randomness and avoiding stagnation.

$$P(u) = \frac{\exp(\mathcal{D}_u)}{\sum_{\tilde{u} \in U \setminus \tilde{U}, A_{\tilde{u}}=1} \exp(\mathcal{D}_{\tilde{u}})}, \forall u \in U \setminus \tilde{U} \text{ and } A_u = 1, \quad (3)$$

Here, \mathcal{D}_u represents the aggregate distances from each UAV

Algorithm 2: UAV Deployment Algorithm

Input: $U, V, R_{max}^{A2G}, R_{max}^{A2A}, R_{MHC}$
Output: \tilde{U}

- 1 ▷ **Process 1**
- 2 $A_u \leftarrow 1, \forall u \in U; \tilde{U} \leftarrow \emptyset;$
- 3 Compute $B_{v,u}$ and $D_{u,\tilde{u}}$, $\forall v \in V, \forall v \in r, \forall u, \tilde{u} \in U;$
- 4 Update C and E based on A, B , and D ;
- 5 ▷ **Process 2**
- 6 **while** \tilde{U} does not satisfy Equation 2 **do**
- 7 Select a new UAV $u \in U$ by executing Equation 3;
- 8 **for** $\forall \tilde{u} \in U$ **do**
- 9 **if** $A_{\tilde{u}} = 1 \text{ &&} D_{u,\tilde{u}} \leq R_{MHC}$ **then**
- 10 Use Algorithm 1 to determine whether \tilde{u} is redundant for U ;
- 11 **if True** **then**
- 12 | Add \tilde{u} to \tilde{U} ;
- 13 **else**
- 14 | Re-evaluate considering \tilde{u} as the new UAV;
- 15 **end**
- 16 **end**
- 17 **end**
- 18 Remove \tilde{U} from U ; Add u to \tilde{U} ;
- 19 **end**
- 20 ▷ **Process 3**
- 21 **while** not all $\tilde{u} \in \tilde{U}$ have been evaluated **do**
- 22 Select an unevaluated $u \in \tilde{U}$;
- 23 Use Algorithm 1 to determine whether u is redundant for \tilde{U} ;
- 24 **if True** **then**
- 25 | Remove u from \tilde{U} ;
- 26 **end**
- 27 **end**
- 28 **return** \tilde{U} ;

$u \in U \setminus \tilde{U}$ to the sets of vehicles V and reserved UAVs \tilde{U} .

Algorithm 1 evaluates the redundancy of UAVs within a radius R_{MHC} of the selected UAV u . Redundancy is determined by assessing whether the removal of a UAV compromises the K -fault tolerance among vehicle pairs. If all evaluated UAVs are redundant, they are deactivated in matrix A , and the selected UAV u is added to the set of reserved UAVs \tilde{U} . When a non-redundant UAV \tilde{u} is identified, it remains active and is added to \tilde{U} . The process then assesses redundancy within radius R_{MHC} of \tilde{u} . This process continues until \tilde{U} satisfies all conditions specified in Equation 2.

Process 3: To minimize the number of UAVs while meeting the criteria, each UAV in \tilde{U} is evaluated for redundancy. UAVs are randomly selected from \tilde{U} for evaluation. Non-redundant UAVs are retained, while redundant ones are removed from \tilde{U} and deactivated in matrix A . This process continues until all UAVs in \tilde{U} are assessed. The final \tilde{U} represents the optimal UAV configuration.

Algorithm 2 presents a detailed pseudocode for the proposed UAV deployment heuristic.

IV. FAULT TOLERANCE TOPOLOGY CONTROL ALGORITHM

Our fault tolerant topology control algorithm reduces UAV energy consumption by optimizing the A2A and A2G communication radii for each deployed UAV $u \in \tilde{U}$, ensuring K -fault tolerance between any two vehicles $v, \tilde{v} \in V$.

To substantiate the algorithm's uniqueness and facilitate subsequent proofs, we initially assign weights to each link in the graph G .

Definition 1: For any two directed links $\langle a_1, b_1 \rangle$ and $\langle a_2, b_2 \rangle \in E(G)$, the weight function W satisfies:

$$\begin{aligned} W(a_1, b_1) > W(a_2, b_2) \Leftrightarrow \\ & (D/B)_{a_1, b_1} > (D/B)_{a_2, b_2} \quad || \\ & (D/B)_{a_1, b_1} = (D/B)_{a_2, b_2} \& id(a_1) > id(a_2) \quad || \\ & (D/B)_{a_1, b_1} = (D/B)_{a_2, b_2} \& id(a_1) = id(a_2) \& \\ & id(b_1) > id(b_2) \end{aligned} \quad (4)$$

Here, $id(a)$ and $id(b)$ denote the serial numbers of nodes a and b , such as their IP or MAC addresses. This designation ensures each directed link in G_0 has a unique weight, including pairs $\langle a, b \rangle$ and $\langle b, a \rangle$. Additionally, we specify that the weight assigned to any A2G link exceeds that of any A2A link.

A. FTTCA

The FTTCA process is outlined below.

- 1) For each UAV $u \in \tilde{U}$, calculate the set of one-hop neighbors $N_G(u)$ and $N_A(u)$ in G_0 .
- 2) Determine the vehicles in $N_G(u)$ that belong to $N_G^F(u)$ and the UAVs in $N_A(u)$ that belong to $N_A^F(u)$. $\forall v \in N_G(u), \forall v \in r$, if there exist at least K disjoint paths $pd_{1 \sim K}$ with internal nodes satisfying $pd_i \cap pd_j = \{u, v\}, \forall i, j \in [1, K], i \neq j$ and $W(u, b) < W(u, v), \forall \langle a, b \rangle \in E(pd_{1 \sim K})$, then $v \notin N_G^F(u)$; otherwise, $v \in N_G^F(u)$. Similarly, $\forall \tilde{u} \in N_A(u)$, if there exist at least K disjoint paths $pd_{1 \sim K}$ satisfying $pd_i \cap pd_j = \{u, \tilde{u}\}, \forall i \neq j$ and $W(u_i, u_j) < W(u, \tilde{u}), \forall \langle u_i, u_j \rangle \in E(pd_{1 \sim K})$, then $\tilde{u} \notin N_A^F(u)$; otherwise, $\tilde{u} \in N_A^F(u)$.
- 3) $\forall u \in \tilde{U}, R_u^{A2G} = \max(B_{v,u} \mid \forall v \in N_G^F(u))$ and $R_u^{A2A} = \max(D_{u,\tilde{u}} \mid \forall \tilde{u} \in N_A^F(u))$.

B. Analysis of K -Fault Tolerance

The following proof demonstrates that the FTTCA ensures K -fault tolerance in G_F .

Initially, G_0 is formed by each UAV using R_{max}^{A2A} and R_{max}^{A2G} , while G_F is formed by each UAV adjusting its A2A and A2G communication radii. Note that $V(G_F) = V(G_0)$ and $E(G_F) \subseteq E(G_0)$, with changes in $E(G_F)$ occurring only in some links of $E(G_0)$.

Assuming G_F results from severing t links in G_0 , where $t \geq 0$, the sequence of these breaks doesn't alter G_F 's structure. For clarity, we assume these broken links are ordered

by descending weight, with e_i being the i th heaviest of the t severed links. Let G_i denote G_0 after removing e_i . The transformation from G_0 to G_F proceeds as follows:

$$G_0 \xrightarrow{\text{Disconnect } e_1} G_1 \xrightarrow{\text{Disconnect } e_2} G_2 \dots \xrightarrow{\text{Disconnect } e_t} G_t = G_F \quad (5)$$

where $W(e_i) > W(e_{i+1})$, $V(G_i) = V(G_{i+1})$, $E(G_{i+1}) = E(G_i) - e_{i+1} = E(G_0) - \{e_1, e_2, \dots, e_{i+1}\}$, $\forall i \in [0, t-1]$.

Lemma 1: Given FTTCA, for $e_{i+1} = \langle a, b \rangle, \forall i \in [0, t-1]$, there are at least K disjoint paths $pd_{1 \sim K}$, such that $a \Rightarrow b$ in G_{i+1} .

Proof 1: Under FTTCA, if a disconnects $\langle a, b \rangle$, implying $b \notin N_A^F(a) \cup N_G^F(a)$, there are at least K disjoint paths $pd_{1 \sim K}$, such that $a \Rightarrow b$ in G_i . Moreover, $\forall \langle \tilde{a}, \tilde{b} \rangle \in pd_{1 \sim K}, W(\tilde{a}, \tilde{b}) < W(a, b)$ holds. The process ensures links weaker than $\langle a, b \rangle$ are not disrupted in G_{i+1} , thus maintaining the existence of these K paths in G_{i+1} .

Theorem 2: Based on the FTTCA, if $v \Rightarrow \tilde{v}$ exhibits K -vertex fault tolerance in G_0 , then $v \Rightarrow \tilde{v}$ in G_F also possesses K -vertex fault tolerance.

Proof 2: Since t is finite, the proof is conducted using mathematical induction.

- 1) Base case: The theorem holds when $v \Rightarrow \tilde{v}$ in G_0 exhibits K -vertex fault tolerance $\forall v, \tilde{v} \in V, \forall v \in r, \forall \tilde{v} \in \tilde{r}$.
- 2) Inductive assumption: $\forall v, \tilde{v} \in V, \forall v \in r, \forall \tilde{v} \in \tilde{r}$, assume $v \Rightarrow \tilde{v}$ in G_i possesses K -vertex fault tolerance.
- 3) Inductive step: The following proof demonstrates $\forall v, \tilde{v} \in V, \forall v \in r, \forall \tilde{v} \in \tilde{r}, v \Rightarrow \tilde{v}$ possesses K -vertex fault tolerance in G_{i+1} . Let $e_{i+1} = \langle a, b \rangle$, indicating $G_{i+1} = G_i - \langle a, b \rangle$, and let $\{a, b\} \cap \{v, \tilde{v}\} = \emptyset$. The proof for other situations follows a similar approach. If $v \Rightarrow \tilde{v}$ in G_i exhibits K -vertex fault tolerance, it remains connected even after removing any $K-1$ UAVs, denoted as $\hat{U} = \{u_1, \dots, u_{K-1}\}$, and their associated links in G_i . After this removal, the path $v \Rightarrow \tilde{v}$ in G_i becomes p , and $u_k \notin V(p), \forall k \in [1, K-1]$. If $\langle a, b \rangle \notin p$, then removing \hat{U} and their associated links in G_{i+1} does not eliminate the path p for $v \Rightarrow \tilde{v}$, thus supporting the theorem. If $\langle a, b \rangle \in p$, then $a, b \notin \hat{U}$. After removing \hat{U} and their associated links in G_i , the path $v \Rightarrow \tilde{v}$ remains intact as p with $\langle a, b \rangle \in p$. Since $G_{i+1} = G_i - \langle a, b \rangle$, even after removing \hat{U} and their associated links in G_{i+1} , the paths $v \Rightarrow a$ and $b \Rightarrow \tilde{v}$ still exist. According to Lemma 1, at least K disjoint paths $pd_{1 \sim K}$, exist from a to b in G_{i+1} . Therefore, even if $\hat{U} \subset \bigcup_{j=1}^t V(pd_j) - \{a\} - \{b\}$, $v \Rightarrow \tilde{v}$ still holds in G_{i+1} . \square

Theorem 3: Based on FTTCA, if $v \Rightarrow \tilde{v}$ exhibits K -edge fault tolerance in G_0 , then $v \Rightarrow \tilde{v}$ in G_F also possesses K -edge fault tolerance.

Proof 3: Since t is finite, the proof is conducted using mathematical induction.

- 1) Base case: The theorem holds when $v \Rightarrow \tilde{v}$ in G_0 exhibits K -edge fault tolerance $\forall v, \tilde{v} \in V, \forall v \in r, \forall \tilde{v} \in \tilde{r}$.

- 2) Inductive assumption: $\forall v, \tilde{v} \in V$, $\forall v \in r$, $\forall \tilde{v} \in \tilde{r}$, assume $v \Rightarrow \tilde{v}$ in G_i possesses K -edge fault tolerance.
- 3) Inductive step: The following proof demonstrates $\forall v, \tilde{v} \in V$, $\forall v \in r$, $\forall \tilde{v} \in \tilde{r}$, $v \Rightarrow \tilde{v}$ possesses K -edge fault tolerance in G_{i+1} . Let $e_{i+1} = \langle a, b \rangle$, indicating $G_{i+1} = G_i - \langle a, b \rangle$, and let $\{a, b\} \cap \{v, \tilde{v}\} = \emptyset$. The proof for other situations follows a similar approach. If $v \Rightarrow \tilde{v}$ in G_i exhibits K -edge fault tolerance, it remains connected even after breaking any $K-1$ links, denoted as $\hat{L} = \{\langle a_1, b_1 \rangle, \dots, \langle a_{K-1}, b_{K-1} \rangle\}$. If the path from v to \tilde{v} in G_i is denoted as p , then it satisfies $\langle a_k, b_k \rangle \notin V(p)$, $\forall k \in [1, K-1]$. If $\langle a, b \rangle \notin p$ and \hat{L} are broken, the path p from v to \tilde{v} still exists, thus proving the theorem. If $\langle a, b \rangle \in p$, then $\langle a, b \rangle \notin \hat{L}$. Since a path p from v to \tilde{v} exists in G_i after removing \hat{L} with $\langle a, b \rangle \in p$, and $G_{i+1} = G_i - \langle a, b \rangle$, the paths $v \Rightarrow a$ and $b \Rightarrow \tilde{v}$ remain intact in G_{i+1} after removing \hat{L} . According to Lemma 1, there are at least K disjoint paths $pd_{1 \sim K}$, from a to b in G_{i+1} . Therefore, even if $\hat{L} \subset \bigcup_{j=1}^K E(pd_j)$, the path $v \Rightarrow \tilde{v}$ still holds in G_{i+1} . \square

Theorem 4: Based on FTTCA, if $v \Rightarrow \tilde{v}$ exhibits K paths in G_0 , then $v \Rightarrow \tilde{v}$ in G_F also possesses K paths.

Proof 4: Since t is finite, the proof is conducted using mathematical induction.

- 1) Base case: The theorem holds when $v \Rightarrow \tilde{v}$ in G_0 exhibits K paths $\forall v, \tilde{v} \in V$, $\forall v \in r$, $\forall \tilde{v} \in \tilde{r}$.
- 2) Inductive assumption: $\forall v, \tilde{v} \in V$, $\forall v \in r$, $\forall \tilde{v} \in \tilde{r}$, assume $v \Rightarrow \tilde{v}$ in G_i possesses K paths.
- 3) Inductive step: The following proof demonstrates $\forall v, \tilde{v} \in V$, $\forall v \in r$, $\forall \tilde{v} \in \tilde{r}$, $v \Rightarrow \tilde{v}$ possesses K paths in G_{i+1} . Let $e_{i+1} = \langle a, b \rangle$, indicating $G_{i+1} = G_i - \langle a, b \rangle$, and let $\{a, b\} \cap \{v, \tilde{v}\} = \emptyset$. The proof for other situations follows a similar approach. Assume there are at least K paths $p_{1 \sim K}$ from v to \tilde{v} in G_i . If $\langle a, b \rangle \notin p_{1 \sim K}$, then the theorem holds. Otherwise, assume $\langle a, b \rangle \in p_1$. Represent p_1 as $p_{va} \bowtie \langle a, b \rangle \bowtie p_{b\tilde{v}}$, where p_{va} is the path from v to a and $p_{b\tilde{v}}$ is the path from b to \tilde{v} in p_1 . Since $G_{i+1} = G_i - \langle a, b \rangle$, p_{va} and $p_{b\tilde{v}}$ still exist in G_{i+1} . According to Lemma 1, there exist at least K disjoint paths $pd_{1 \sim K}$, from a to b . Consequently, in G_{i+1} , there are at least K paths from v to \tilde{v} where duplicate nodes may appear: $p_{va} \bowtie pd_{1 \sim K} \bowtie p_{b\tilde{v}}$. Since p_1 is a path in G_i , the path $p_{va} \bowtie \langle a, b \rangle \bowtie p_{b\tilde{v}}$ does not have any common points. Furthermore, since $pd_{1 \sim K}$ are K disjoint paths in G_{i+1} , these paths can still be formed by removing loops from paths that may contain duplicate nodes. Therefore, there are at least K paths from v to \tilde{v} in G_{i+1} . \square

V. EVALUATION AND RESULTS

To the best of our knowledge, fault tolerance in UAV-assisted vehicular networks remains unexplored in existing literature. Consequently, our study focuses on evaluating the effectiveness of the proposed fault tolerance mechanism for UAV and link failures, along with the feasibility of UAV deployment and topology control algorithms.

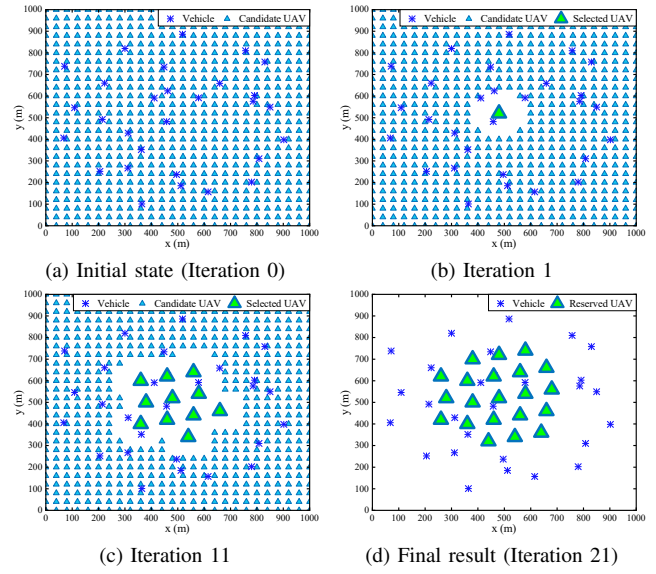


Fig. 3: The first step of UAV deployment algorithm where $K = 1$. (Illustrated in a $1\text{km} \times 1\text{km}$ area.)

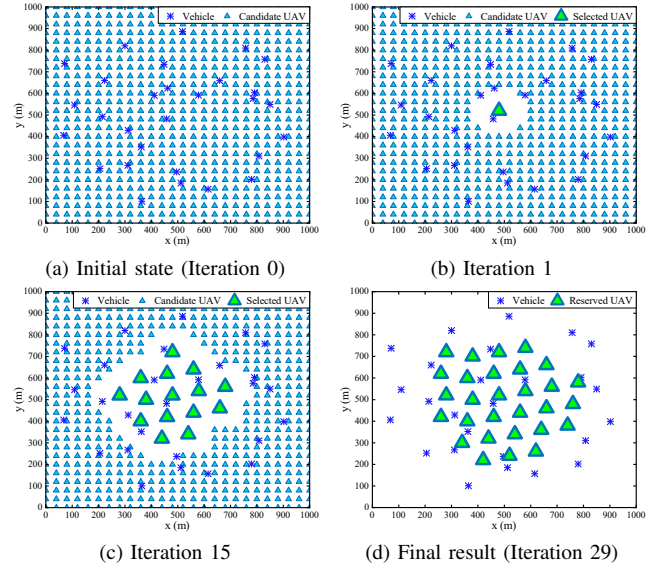


Fig. 4: The first step of UAV deployment algorithm where $K = 2$. (Illustrated in a $1\text{km} \times 1\text{km}$ area.)

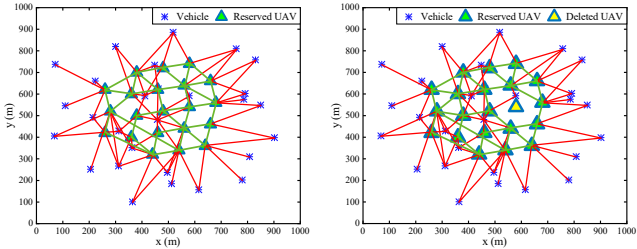
A. Evaluation Setup

Our simulation models a UAV-assisted vehicular network in a $20 \times 20 \text{ km}^2$ disaster zone, with a vehicle density of 30 vehicles/ km^2 [14]. Each vehicle is assigned a search and rescue operation radius of 50 m. Table II provides a comprehensive list of the simulation parameters.

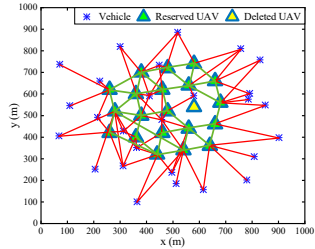
TABLE II: Primary Simulation Parameters

Symbol	Value	Symbol	Value
Z	300 m [14]	δ	$\frac{\pi}{4}$ [11]
P_s	30 dBm [9]	R_{max}^{A2A}	500 m [9]
R_{MHC}	100 m [12]	f_0	2 GHz [9]
c	$3 \times 10^8 \text{ m/s}$	K	1, 2, 3, 4

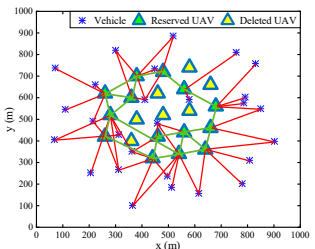
Specifically, $K = 1$ represents no fault tolerance, while $K = 2, 3$, and 4 indicate increasing levels of fault tolerance.



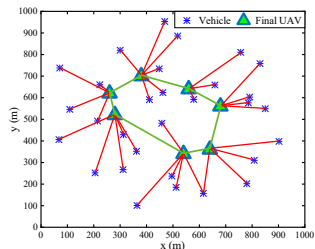
(a) Initial state (Iteration 0)



(b) Iteration 1



(c) Iteration 7



(d) Final result (Iteration 14)

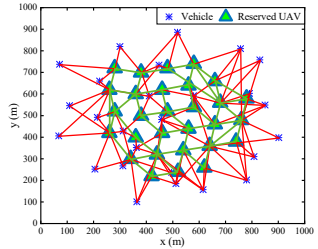
Fig. 5: The second step of UAV deployment algorithm where $K = 1$. (Illustrated in a $1\text{km} \times 1\text{km}$ area.)

B. Main Results

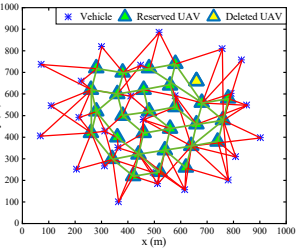
Figures 3 and 4 depict the iterative process and final results of the initial UAV deployment phase for $K = 1$ and 2. Figures 3a and 4a show the initial random vehicle placement, with UAVs positioned at each grid intersection. Figures 3b, 3c, 4b, and 4c illustrate the progressive elimination of redundant UAVs for each fault tolerance level, with links omitted for clarity. Active UAVs are retained while redundant ones are eliminated. Figures 3c and 4c demonstrate that by the 11th and 15th iterations, 11 and 15 UAVs are retained, respectively. The process concludes at the 21st and 29th iterations, with 21 and 29 UAVs remaining for $K = 1$ and 2, respectively.

Figures 5 and 6 depict the iterative process and final results of the second phase UAV deployment for $K = 1$ and 2. Figures 5a and 6a show the final UAV distributions from the first phase, correlating with Figures 3d and 4d. Selected A2G (red) and A2A (green) links are shown for clarity. The second phase involves iterative removal of redundant UAVs. Figures 5c and 6c demonstrate that 7 and 15 UAVs are eliminated after iterations, respectively. The algorithm concludes after 14 and 19 iterations, with 7 and 10 UAVs remaining for $K = 1$ and 2 respectively, ensuring adequate coverage for all vehicles under the specified fault tolerances. The higher number of UAVs retained for $K = 2$ compared to $K = 1$ reflects the increased fault tolerance requirements defined in Equation 2.

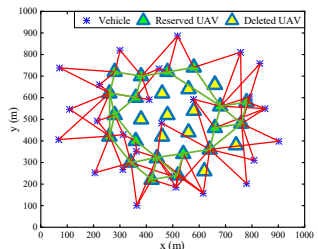
Figure 7 illustrates the FTTCA for fault tolerance levels $K=1, 2$. Figures 7a and 7c depict the final UAV configurations from Figures 5d and 6d, utilizing maximum distances R_{max}^{A2G} and R_{max}^{A2A} for A2G and A2A communications, respectively. These figures display all A2G and A2A links. FTTCA then eliminates redundant A2G and A2A links based on the specified fault tolerance levels, yielding the final network topology shown in Figures 7b and 7d. FTTCA significantly simplifies the network topology, reducing the number of A2G and A2A links per UAV, thus substantially lowering costs.



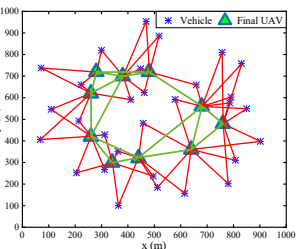
(a) Initial state (Iteration 0)



(b) Iteration 1

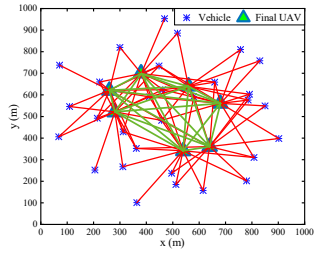


(c) Iteration 10

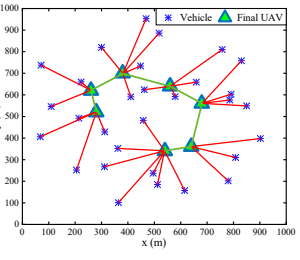


(d) Final result (Iteration 19)

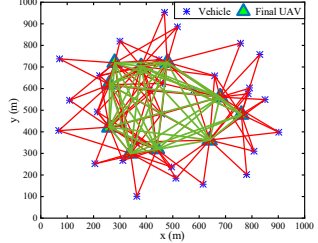
Fig. 6: The second step of UAV deployment algorithm where $K = 2$. (Illustrated in a $1\text{km} \times 1\text{km}$ area.)



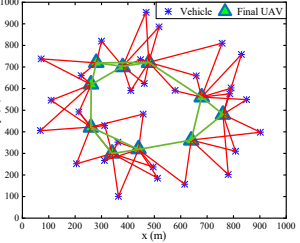
(a) Initial state



(b) Disconnect A2G and A2A links



(c) Initial state



(d) Disconnect A2G and A2A links

Fig. 7: The process of FTTCA algorithm where $K = 1$ (upper section) and $K = 2$ (lower section).

Figures 7b and 7d demonstrate that higher K values result in a moderate increase in UAV numbers and connections, underscoring the trade-off between enhanced fault tolerance and increased system costs.

Figures 8a and 8b illustrate the communication success rate in relation to UAV and link failures. The communication success rate decreases proportionally to the increasing probability of failures. This decline stems from the reduction in available UAVs and operational links, leading to network fragmentation into multiple subnetworks. The efficiency of UAV-assisted vehicular communication decreases as the number of subnetworks increases. Moreover, given equal failure probabilities, networks with higher K values are better able to minimize information island formation and maintain higher

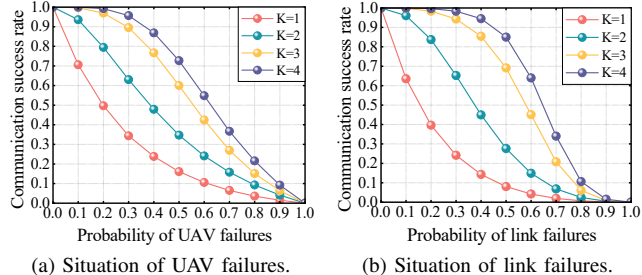


Fig. 8: Evaluating the fault tolerance performance of UAV-assisted vehicular network for UAV failures and link failures.

communication success rates.

VI. RELATED WORK

A. UAV-Assisted Vehicular Networks

Su et al. [5] developed a lightweight, blockchain-based framework for secure data sharing in UAV-assisted vehicular networks during disaster rescues. Liao et al. [15] proposed energy-efficient 3D UAV deployment for interchange bridges. Tan et al. [16] presented a UAV-based certificateless group authentication for secure data transmission in infrastructure-less IoT.

B. UAV Deployment Algorithms

Zhang et al. [17] used particle swarm optimization for optimal 3D UAV placement based on coverage probability. Wang et al. [18] integrated centralized greedy search and distributed motion strategies for dynamic UAV deployment covering ground users. Zhang et al. [19] proposed a multi-virtual force sharing UAV deployment strategy for improved coverage with limited UAVs and mobile users.

C. Topology Control Algorithms

Le Huu et al. [20] proposed TFACR, a topology control algorithm matching node degrees to desired levels for improved network performance. Ding et al. [21] developed an energy-efficient topology control method for IoT, maximizing efficiency during adjustments. Yoo et al. [22] created a UAV network topology control system, optimizing connectivity, interference, and energy use for better throughput and efficiency.

Despite advancements in UAV-assisted vehicular networks, UAV deployment algorithms, and topology control algorithms, a significant gap persists in fault tolerance. Current solutions inadequately address UAV or link failures, potentially compromising network integrity and performance.

VII. CONCLUSION

This study presents a fault tolerance mechanism to improve communication reliability in UAV-assisted vehicular networks during emergencies. We propose a K -fault tolerance approach and develop a UAV deployment algorithm that minimizes costs while ensuring fault tolerance. Furthermore, we introduce the FTTCA, which optimizes UAV communication ranges to achieve cost-effective K -fault tolerance. Simulation results demonstrate the efficacy of the proposed UAV deployment

algorithm and FTTCA, which outperform existing methods in managing UAV and link failures.

REFERENCES

- [1] A. Pal, J. Wang, Y. Wu, K. Kant, Z. Liu, and K. Sato, "Social media driven big data analysis for disaster situation awareness: A tutorial," *IEEE Transactions on Big Data*, vol. 9, no. 1, pp. 1–21, 2023.
- [2] Z. Xie, Y. Chen, I. Ali, C. Pan, F. Li, and W. He, "Efficient and secure certificateless signcryption without pairing for edge computing-based internet of vehicles," *IEEE Transactions on Vehicular Technology*, vol. 72, no. 5, pp. 5642–5653, 2023.
- [3] M. Matracia, M. A. Kishk, and M.-S. Alouini, "Uav-aided post-disaster cellular networks: A novel stochastic geometry approach," *IEEE Transactions on Vehicular Technology*, vol. 72, no. 7, pp. 9406–9418, 2023.
- [4] H. Shakhatreh, A. Kheirshah, and B. Ji, "Uavs to the rescue: Prolonging the lifetime of wireless devices under disaster situations," *IEEE Trans. Green Commun. Netw.*, vol. 3, no. 4, pp. 942–954, 2019.
- [5] Z. Su, Y. Wang, Q. Xu, and N. Zhang, "LVBS: lightweight vehicular blockchain for secure data sharing in disaster rescue," *IEEE Trans. Dependable Secur. Comput.*, vol. 19, no. 1, pp. 19–32, 2022.
- [6] M. Marcozzi, O. Gemikonakli, E. Gemikonakli, E. Ever, and L. Mostarda, "Availability evaluation of iot systems with byzantine fault-tolerance for mission-critical applications," *Internet Things*, vol. 23, p. 100889, 2023.
- [7] K. Pan, "Star fault tolerance of hypercube," *Theor. Comput. Sci.*, vol. 972, p. 114052, 2023.
- [8] Y. Zeng, R. Zhang, and T. J. Lim, "Wireless communications with unmanned aerial vehicles: opportunities and challenges," *IEEE Commun. Mag.*, vol. 54, no. 5, pp. 36–42, 2016.
- [9] H. Zhao, H. Wang, W. Wu, and J. Wei, "Deployment algorithms for UAV airborne networks toward on-demand coverage," *IEEE J. Sel. Areas Commun.*, vol. 36, no. 9, pp. 2015–2031, 2018.
- [10] M. Alzenad and H. Yanikomeroglu, "Coverage and rate analysis for unmanned aerial vehicle base stations with los/nlos propagation," in *IEEE Globecom Workshops, GC Wkshps 2018, Abu Dhabi, United Arab Emirates, December 9–13, 2018*, 2018, pp. 1–7.
- [11] M. Liu, J. Yang, and G. Gui, "DSF-NOMA: uav-assisted emergency communication technology in a heterogeneous internet of things," *IEEE Internet Things J.*, vol. 6, no. 3, pp. 5508–5519, 2019.
- [12] J. Lyu and H. Wang, "Secure UAV random networks with minimum safety distance," *IEEE Trans. Veh. Technol.*, vol. 70, no. 3, pp. 2856–2861, 2021.
- [13] M. Haenggi, *Stochastic geometry for wireless networks*. Cambridge University Press, 2012.
- [14] S. Zhang, Y. Zhu, and J. Liu, "Multi-uav enabled aerial-ground integrated networks: A stochastic geometry analysis," *IEEE Trans. Commun.*, vol. 70, no. 10, pp. 7040–7054, 2022.
- [15] Z. Liao, Y. Ma, J. Huang, and J. Wang, "Energy-aware 3d-deployment of UAV for iov with highway interchange," *IEEE Trans. Commun.*, vol. 71, no. 3, pp. 1536–1548, 2023.
- [16] H. Tan, W. Zheng, and P. Vijayakumar, "Secure and efficient authenticated key management scheme for uav-assisted infrastructure-less iots," *IEEE Trans. Intell. Transp. Syst.*, vol. 24, no. 6, pp. 6389–6400, 2023.
- [17] Y. Zhang, L. Zhang, and L. Chunpeng, "3-d deployment optimization of uavs based on particle swarm algorithm," in *19th IEEE International Conference on Communication Technology, ICCT 2019, Xi'an, China, October 16–19, 2019*. IEEE, 2019, pp. 954–957.
- [18] H. Wang, H. Zhao, W. Wu, J. Xiong, D. Ma, and J. Wei, "Deployment algorithms of flying base stations: 5g and beyond with uavs," *IEEE Internet Things J.*, vol. 6, no. 6, pp. 10 009–10 027, 2019.
- [19] S. Zhang, D. Wu, L. Jiang, X. Jin, and S. Cen, "Research on UAV access deployment algorithm based on improved virtual force model," *KSII Trans. Internet Inf. Syst.*, vol. 16, no. 8, pp. 2606–2626, 2022.
- [20] L. H. Binh, T.-V. T. Duong, and V. M. Ngo, "Tfacr: A novel topology control algorithm for improving 5g-based manet performance by flexibly adjusting the coverage radius," *IEEE Access*, vol. 11, pp. 105 734–105 748, 2023.
- [21] Z. Ding, L. Shen, H. Chen, F. Yan, and N. Ansari, "Energy-efficient topology control mechanism for iot-oriented software-defined wsns," *IEEE Internet of Things Journal*, vol. 10, no. 15, pp. 13 138–13 154, 2023.
- [22] T. Yoo, S. Lee, K. Yoo, and H. Kim, "Reinforcement learning based topology control for uav networks," *Sensors*, vol. 23, no. 2, 2023.